Functionally enhanced placenta-derived mesenchymal stem cells inhibit adipogenesis in orbital fibroblast with graves' ophthalmopathy

Jae Yeon Kim
CHA University
Sohae Park
CHA University
Hyun-Jung Lee
CHA University
Helen Lew
CHA Bundang Medical Center
Gi Jin Kim (gjkim@cha.ac.kr)
CHA University https://orcid.org/0000-0002-2320-7157

Research

Keywords: Adipogenesis, Graves' ophthalmopathy, Gene modification, Phosphatase of regenerating liver-1, Placenta-derived mesenchymal stem cells

Posted Date: February 19th, 2020

DOI: https://doi.org/10.21203/rs.2.23922/v1

Version of Record: A version of this preprint was published on November 5th, 2020. See the published version at https://doi.org/10.1186/s13287-020-01982-3.

Abstract

Background: Placenta-derived mesenchymal stem cells (PD-MSCs) have unique immunomodulatory properties, and Phosphatase of regenerating liver-1 (PRL-1) regulates self-renewal ability of stem cells and promotes proliferation. Graves' ophthalmopathy (GO) is an autoimmune inflammatory disease of the orbit and is characterized by increased orbital contents involving adipose tissue. Because the mechanism of inhibiting adipogenesis in orbital fibroblast (OF) with GO patients remains uncertain, the major objective is to investigate mechanisms alleviating adipogenesis by PRL-1 overexpressing PD-MSCs (PD-MSCsPRL-1, PRL-1+) in OF derived from GO patients. Methods: primary OFs from patients with GO were isolated from orbital adipose tissue specimens. After maturation as adipogenic differentiation, normal and GO-derived OF were cocultured with naïve and PD-MSCsPRL-1. Western blotting were conducted for evaluating molecular mechanisms for inhibiting adipogenesis in GO. Results: The characterizations of PD-MSCsPRL-1 were similar to naïve. OF with GO patients stimulated adipocyte differentiation were significantly decreased lipid accumulation by cocultivation with PD-MSCsPRL-1 comparing with naïve. The mRNA and protein expression of adipogenic markers was declined in PD-MSCsPRL-1. The expression of pPI3K/AKT/mTOR protein in OF with GO patients was downregulated by cocultivation with PD-MSCsPRL-1 secreted IGFBPs. Interestingly, IGFBP2, 4, and 7 expressions through integrin alpha 4 (ITGA4) and beta 7 (ITGB7) in PD-MSCsPRL-1 were higher than naïve and upregulated pFAK downstream factor. Conclusion: Taken together, secreted IGFBPs by PD-MSCsPRL-1 via upregulating FAK and blocking IGF inhibit adipogenesis of OF with GO patients, providing novel therapeutic approach using functionally enhanced MSCs potential for degenerative diseases.

Background

Graves' ophthalmopathy (GO) is a thyroid autoimmune, potentially sight-threatening ocular disease. The main symptoms of GO comprise proptosis impairment of eye motility, lid retraction, de novo adipogenesis, and soft tissue inflammation. Especially, inflammatory reactions of orbital fibroblast (OF) are responsible for these symptoms in the disease [1]. Consideration of any involvement of insulin-like growth factor 1 receptor (IGF-1R) in GO suggested substantial evidence [2]. TSHR and IGF-1R in OF surface receptors both stimulate hyaluronic synthesis and de novo adipogenesis by peroxisome proliferator-activated receptor gamma (PPAR-γ) [3, 4].

Based on the molecular pathogenesis, medical and surgical treatment to patients with GO has been implemented. Especially, corticosteroids and orbital radiotherapy continue to be the medical therapy for patients with GO [5]. To reduce compressive optic neuropathy in patients with active thyroid eye disease, response to orbital radiotherapy combined with corticosteroids was protective against disease progression [6]. However, glucocorticoid therapy to patients has negative effect of hyperthyroid status on adrenal insufficiency as well as acute liver damage following alanine aminotransferase 300 U/L over [7, 8]. Moreover, other medical radiotherapy also resulted in developing malignancies according to age and gender of patients [9].

Placenta-derived mesenchymal stem cells (PD-MSCs) have been broadly investigated due to multi-lineage differentiation potential, especially potent immune modulation ability for tissue repair and regenerative medicine. MSCs inhibit cell proliferation of T, B, Natural killer, and dendritic cells. Due to these immune regulatory properties, the safety and clinical efficacy of MSC-based therapy has been tested in autoimmune disorders including rheumatoid arthritis, graft-versus-host-disease (GVHD) [10]. PD-MSCs suppressed the responses of mitogen-stimulated T cell proliferation as well as decreased IL-12, TNF-α, and IFN-γ in vivo model with GVHD [11]. In comparison to other MSCs, PD-MSCs have additional advantage of immunomodulatory function by regulating expression of human leukocyte antigens (HLA)-ABC and –G [12]. Hence, therapeutic effects of PD-MSCs were considered to immunosuppressive potentials to replace the damaged tissues.

Phosphatase of regenerating liver-1 (PRL-1), known as protein tyrosine phosphatase type IVA, member 1 (PTP4A1); PTPCAAX1, is a member of a small class of prenylated PTPs. PRL-1 was originally identified as immediate early gene during liver regeneration [13]. PRL-1 contained C-terminal prenylation motif for farnesylation CAAX [14]. PRL-1 promotes cellular proliferation during protein prenylation, which is post translational lipid modification process, by upregulating RhoA via mevalonate metabolic pathway. The major enzyme HMG-CoA reductase during protein prenylation regulates AMPK by PRL-1 [15]. Moreover, PRL-1 modulates oxidative-stress response in mammalian retina [16]. PRL-2, which is PRL-1 same class of subfamily with similar amino acid sequences, plays an important role for hematopoietic stem cell self-renewal.

Recently, we reported therapeutic effects by application of naïve PD-MSCs in a GO mice model [17]. However, it is still unknown whether functionally enhanced PRL-1 in PD-MSCs (PD-MSCs^{PRL-1}, PRL-1+) inhibits adipogenesis in OF with GO patients as molecular mechanism to provide a therapeutic efficacy.

Materials And Methods

Cell culture and gene transfection

Orbital adipose tissue specimens were obtained from patients with GO (n = 3) during fat decompression and control individuals without GO history (n = 3) under the consent conditions. Orbital fibroblast preparation was approved by Institutional Review Board of CHA Bundang Medical Center, Seongnam, Republic of Korea. Orbital tissue explants were chopped and treated with 0.25 mg/mL collagenase (Sigma-Aldrich, St. Louis, MO, USA) for 1 h at 37℃ shaking incubator. After collagenase digestion, the orbital tissues were placed in the culture plates with DMEM/F12 supplemented 20% fetal bovine serum (FBS; Gibco, Carlsbad, CA, USA), and 1% penicillin/streptomycin (P/S; Gibco).

Placentas were collected for research purposes by the Institutional Review Board of CHA Gangnam Medical Center, Seoul, KOREA (IRB 07–18). PD-MSCs were isolated as described previously [18] and cultured in α-modified minimal essential medium (α-MEM; Hyclone Logan, UT, USA) supplemented with 10% FBS (Gibco), 1% P/S (Gibco), 1 μg/mL heparin (Sigma-Aldrich), and 25 ng/mL human fibroblast

growth factor-4 (hFGF-4; Peprotech, Rocky Hill, NJ, USA). PRL-1 (protein tyrosine phosphatase type IVA, member 1; PTP4A1) plasmid vector was purchased (#RG200435; Origene, Rockville, MD, USA). To induced overexpression of PRL-1 gene, naïve PD-MSCs (passage = 7) transfected using AMAXA Nucleofector system (Lonza, Basel, Switzerland) according to the manufacturer's instructions. After transfection for 24 h, cells were selected by 1.5 mg/mL neomycin. All kinds of cells were maintained at 37°C in humidified atmosphere containing 5% CO_2.

Differentiation for PD-MSCs^{PRL-1} and OF with GO

To analyze the potential of PD-MSCs^{PRL-1} to differentiate into mesodermal lineages, PD-MSCs^{PRL-1} (passage = 5) were plated at density of 5×10^3 cells/cm^2 in each differentiation induction medium using StemPro Adipogenesis and Osteogenesis differentiation kit (Gibco) according to the manufacturer's instructions. After approximately 21 days, PD-MSCs^{PRL-1} were fixed in 4% paraformaldehyde and incubated for 1 h with Oil Red O (Sigma-Aldrich) for staining lipids to visualize lipid vesicles and von Kossa staining with 5% silver nitrate (Sigma-Aldrich) under light to evaluate their accumulation of calcium deposits.

To induce adipogenic differentiation, normal and GO-derived orbital fibroblasts (5×10^3 cells/cm^2) were seeded and changed to serum-free DMEM/F12 supplemented with 33 μM biotin, 17 μM pantothenic acid, 10 μg/mL transferrin, 0.2 nM triiodothyronine (T_3), 1 μM insulin (all from Sigma-Aldrich), 0.2 μM carbaprostacyclin ($cPGI_2$; Cayman Chemical, Ann Arbor, MI, USA), 1 μM dexametasone, and 0.1 mM isobutylmethylxanthine (IBMX; all from Sigma-Aldrich) for the first 4 days only. To induce maturation of adipogenesis, the medium was supplemented except 1 μM dexamethasone and 0.1 mM IBMX (all from Sigma-Aldrich) for 6 days. The media was replaced every other day. Lipid accumulation and adipocyte morphology were visualized by Oil red O staining.

Coculture experiments

For the detection of inhibition of adipogenesis, normal and GO-derived orbital fibroblasts after adipogenesis differentiation were cocultured with naïve and PD-MSCs^{PRL-1} (5×10^3 cells/cm^2

onto Transwell inserts (8 μM pore size; Corning, NY, USA) in α-MEM (Hyclone) supplemented with 10% FBS and 1% P/S (all from Gibco) for 24 h at 37°C in humidified atmosphere containing 5% CO_2.

Reverse transcription polymerase chain reaction (RT-PCR) and quantitative real time PCR (qRT-PCR)

Total RNA was extracted using TRIzol LS reagent (Invitrogen, Carlsbad, CA) according to the manufacturer's protocol. The concentration and purity of total RNA were determined spectrophotometrically at OD 260 nm and 280 nm. cDNA was synthesized by reverse transcriptase (RT) from total RNA (500 ng) by using SuperScript III reverse transcriptase (Invitrogen). To analyze stemness markers in PD-MSCs^{PRL-1}, PCR amplification was performed with specific primers (Table 1). β-actin was

used as an internal control. Amplified PCR products were electrophoresed on 2% agarose gels containing 1.5 μg/mL ethidium bromide and visualized under UV light. qRT-PCR analysis was used to differences in gene expression. qRT-PCR was performed with primers (Table 2) and SYBR Green PCR Master Mix (Roche, Basel, Switzerland) in CFX Connect™ Real-Time System (Bio-Rad, Hercules, CA, USA). All reactions were performed in triplicate.

Table 1
Primer sequences using reverse transcription polymerase chain reaction

Genes		Primer sequences	Tm
Oct4	Forward	5'-AGTGAGAGGCAACCTGGAGA-3'	52
	Reverse	5'-GTGAAGTGAGGGCTCCCATA-3'	
Nanog	Forward	5'-TTCTTGACTGGGACCTTGTC-3'	52
	Reverse	5'-GCTTGCCTTGCTTTGAAGCA-3'	
Sox2	Forward	5'-GGGCAGCGTGTACTTATCCT-3'	52
	Reverse	5'-AGAACCCCAAGATGCACAAC-3'	
HLA-G	Forward	5'-GCGGCTACTACAACCAGAGC-3'	58
	Reverse	5'-GCACATGGCACGTGTATCTC-3'	
TERT	Forward	5'-GAGCTGACGTGGAAGATGAG-3'	55
	Reverse	5'-CTTCAAGTGCTGTCTGATTCCAATG-3'	
AFP	Forward	5'-ATGCTGCAAACTGACCACGC-3'	55
	Reverse	5'-GCTTCGCTTTGCCAATGCTT-3'	
Albumin	Forward	5'-TGAGTTTGCAGAAGTTTCCA-3'	60
	Reverse	5'-CCTTTGCCTCAGCATAGTTT-3'	
β-actin	Forward	5'-TCCTTCTGCATCCTGTCAGCA-3'	58
	Reverse	5'-CAGGAGATGGCCACTGCCGCA-3'	

Table 2

Primer sequences using quantitative real time polymerase chain reaction

Genes		Primer sequences	Tm
OC	Forward	5'-AGTGAGAGGCAACCTGGAGA-3'	52
	Reverse	5'-GTGAAGTGAGGGCTCCCATA-3'	
COL1A1	Forward	5'-TTCTTGACTGGGACCTTGTC-3'	52
	Reverse	5'-GCTTGCCTTGCTTTGAAGCA-3'	
Adipsin	Forward	5'-GGGCAGCGTGTACTTATCCT-3'	52
	Reverse	5'-AGAACCCCAAGATGCACAAC-3'	
PPAR-γ	Forward	5'-GCGGCTACTACAACCAGAGC-3'	58
	Reverse	5'-GCACATGGCACGTGTATCTC-3'	
Adiponectin	Forward	5'-GAGCTGACGTGGAAGATGAG-3'	55
	Reverse	5'-CTTCAAGTGCTGTCTGATTCCAATG-3'	
Leptin	Forward	5'-ATGCTGCAAACTGACCACGC-3'	55
	Reverse	5'-GCTTCGCTTTGCCAATGCTT-3'	
LPL	Forward	5'-TGAGTTTGCAGAAGTTTCCA-3'	60
	Reverse	5'-CCTTTGCCTCAGCATAGTTT-3'	
FABP4	Forward	5'-GCATGGCCAAACCTAACATGA-3'	55
	Reverse	5'-CCTGGCCCAGTATGAAGGAAA-3'	
IGFBP1	Forward	5'-GAGCCCTGCCGAATAGAAC-3'	60
	Reverse	5'-GGATCCTCTTCCCATTCCAAG-3'	
IGFBP2	Forward	5'-ACATCCCCAACTGTGACAAG-3'	60
	Reverse	5'-ATCAGCTTCCCGGTGTTG-3'	
IGFBP3	Forward	5'-CAGAGCACAGATACCCAGAAC-3'	60
	Reverse	5'-AGCACATTGAGGAACTTCAGG-3'	
IGFBP4	Forward	5'-CTGACAGCTTTCGAGAGTGAG-3'	60
	Reverse	5'-GCGCATTTGAGGGAAACTTC-3'	
IGFBP5	Forward	5'-ACCCAGTCCAAGTTTGTCG-3'	60
	Reverse	5'-TGTAGAATCCTTTGCGGTCAC-3'	

Genes		Primer sequences	Tm
IGFBP6	Forward	5'-GTCTACACCCCTAACTGCG-3'	60
	Reverse	5'-CTCTGTTGGTCTCTGCGG-3'	
IGFBP7	Forward	5'-GCCCAGAAAAGCATGAAGTAAC-3'	60
	Reverse	5'-TTTATAGCTCGGCACCTTCAC-3'	
ITGA4	Forward	5'-AGAGAGACAATCAGTGGTTGG-3'	55
	Reverse	5'-TCAGTTCTGTTCGTAAATCAGG-3'	
ITGB7	Forward	5'-AGCAGCAACAACTCAACTGG-3'	55
	Reverse	5'-TTACAGACCCACCCTTCCTCT-3'	
FAK	Forward	5'-GAAGCATTGGGTCGGGAACTA-3'	55
	Reverse	5'-CTCAATGCAGTTTGGAGGTGC-3'	
GAPDH	Forward	5'-TCCTTCTGCATCCTGTCAGCA-3'	58
	Reverse	5'-CAGGAGATGGCCACTGCCGCA-3'	

Flow cytometry analysis

For immunophenotyping of cell surface antigens, third-passage PD-MSCs^{PRL-1} were detached and stained with fluorescein isothiocyanate- (FITC-) and phycoerythrin- (PE-) conjugated antibodies and were analyzed with FACSablibur flow cytometer (Becton Dickinson, Franklin Lakes, NJ, USA). Monoclonal antibodies against the human antigens CD34-PE, CD90-PE, HLA-ABC-FITC, HLA-DR-FITC (BD Bioscience, San Jose, CA, USA), CD13-PE (BioLegend, San Diego, CA, USA), CD105-FITC (R&D Systems, Minneapolis, MN, USA), and HLA-G (Abcam, Cambridge, UK) were used. For each sample, at least 10,000 events were acquired.

Teratoma formation and histological analysis

Nine-week-old male NOD/SCID mice (Laboratory animal Research Center, Bungdang CHA Medical Center, CHA University, Seongnam, Republic of Korea) were maintained in an air-conditioned animal house under specific pathogen-free conditions. To investigate teratoma formation, PD-MSCs^{PRL-1} (5×10^5 cells) were directly injected into each testis (TP; n = 2). Control mice was not injected (Con; n = 2). After maintaining for 14 weeks, testes were collected and all mice were sacrificed. Testis were homogenized and fixed in 10% Neutral buffered formalin and embedded in paraffin. Sections were stained with haematoxylin and eosin (H&E).

Western blotting

Total protein was acquired by lysis buffer (Sigma-Aldrich). The protein lysates were separated by 8 to 12% sodium dodecyl sulfate polyacrylamide gel electrophoresis (SDS-PAGE), and transferred to

polyvinylidene difluoride (PVDF) membranes, blocked in 5% Bovine serum albumin, and then incubated overnight 4°C with primary antibodies : anti-PI3K p110 alpha (1:1000, Cell Signaling Technology, Denvers, MA), anti-pAKT (1:1000, Cell Signalling Technology), anti-pmTOR (1,1000, Abcam), anti-pFAK (1:1000, Cell Signaling Technology), anti-PPAR-γ (1:500, Santa Cruz Biotechnology, Dallas, TX), anti-leptin (1:500, R&D systems), anti-TNF-α (1:500, Santa Cruz Biotechnology), and anti-GAPDH (1:3000, AbFrontier, Seoul, Republic of Korea). Membranes incubated with horseradish peroxidase- (HRP) conjugated secondary antibodies (Bio-Rad, Hercules, CA, USA). The bands were detected using an enhanced-chemiluminescence reagent (Bio-Rad).

Statistical analysis

The experimental statistics were expressed as the means ± SD. Statistical analysis was performed using Student's t-test, and the difference was considered statistically significant when the p value was less than 0.05. Each experiment has been conducted in duplicate or triplicate.

Results

Characterization of PD-MSCs modified with PRL-1 gene

The PD-MSCs were transfected with PRL-1 gene (PD-MSCs^{PRL-1}, PRL-1+) using non-viral AMMXA system (Fig. 1a). After transfection, PRL-1 expression in PD-MSCs was identified by green fluorescent protein (GFP) reporter gene (Fig. 1b). Expression levels of PRL-1 mRNA and protein in PD-MSCs^{PRL-1} were significantly higher than those in naïve (Fig. 1c, d). To confirm that PD-MSCs^{PRL-1} corresponded to naïve, we observed mRNA expression of genes associated with stemness markers such as Oct4, Nanog and Sox2, and telomerase reverse transcriptase (TERT) and HLA-G. As expected, PD-MSCs^{PRL-1} were well maintained at passage 1 and 6 (Fig. 1e). To identify the phenotypes of PD-MSCs, the cell surface markers of PD-MSCs^{PRL-1} were analyzed by flow cytometry. PD-MSCs^{PRL-1} were positive for the expression of MSC markers, CD13, CD90, and CD105, but negative for the hematopoietic lineage markers CD34 and HLA-DR. However, HLA class I molecules, HLA-ABC was expressed at high level (Fig. 1f). Also, no teratoma formation was observed after transplantation of PD-MSCs^{PRL-1} (Fig. 1G). To further evaluate the differentiation potential of PD-MSCs^{PRL-1} into mesodermal lineage, PD-MSCs^{PRL-1} exposed to osteogenic and adipogenic induction conditions. The osteogenic and adipogenic differentiated cells in PD-MSCs^{PRL-1} were stained positively using von Kossa and Oil red O staining, respectively (Fig. 1h). Previously, we confirmed in naïve MSCs as multi-differentiation potentials [19]. After differentiations, osteogenic-specific markers (Osteocalcin; OC and Collagen Type 1 alpha 1; COL1A1) and adipogenic-specific markers (Adipsin and peroxisome proliferator-activated receptor gamma; PPAR-γ) were expressed at high level in differentiated PD-MSCs^{PRL-1} by qRT-PCR (Fig. 1i, j). These findings suggest that PD-MSCs^{PRL-1} maintain similar characterization of naïve.

PD-MSCs^{PRL-1} inhibit adipogenesis OF with GO patients

To evaluate the effects of PD-MSCs^{PRL-1} on the adipogenesis in OF with GO patients, Normal and GO-derived OFs were induced adipogenesis for the first 4 days to induce adipogenesis and for 6 days to maturation. After 10 days of in vitro maturation, differentiated GO-derived OFs were indirectly cocultured with naïve and PD-MSCs^{PRL-1} (Fig. 2a). Adipogenesis induced normal and GO-derived OFs was stained using Oil Red O to visualize lipid accumulation (Fig. 2b). mRNA expressions of adipogenic-specific markers (adipsin, adiponectin, PPAR-γ, leptin, lipoprotein lipase; LPL, and fatty acid-binding protein 4; FABP4) in OF with GO patients cocultivation with naïve and PD-MSCs^{PRL-1} were decreased compared to non-cocultivation. Interestingly, adiponectin, leptin, and LPL expressions in PD-MSCs^{PRL-1} cocultivation were significantly decreased compared with naïve coculture. Moreover, PPAR-γ, which is transcription factor of de novo adipogenesis in OFs with GO patients, expression in PD-MSCs^{PRL-1} cocultivation was downregulated compared with naïve (Fig. 2c). These finding suggest that PD-MSCs^{PRL-1} downregulate gene expressions of adipogenic markers and inhibit adipogenesis in adipogenesis-induced OFs with GO patients.

PD-MSCs^{PRL-1} promote expression of IGFBP genes

IGFBPs control IGF-1R action by regulating the bioavailability of the IGF-1 and IGF-2 ligands, and have been shown to have an inhibitory effect of adipogenesis in human visceral adipocytes. We previously analyzed that naïve and PD-MSCs^{PRL-1} secreted IGFBPs through multiplex cytokine array (data not shown). Therefore, we investigated whether functionally enhanced PD-MSCs with PRL-1 promote the expression of IGFBPs. qRT-PCR analysis revealed that expression levels of IGFBP-2, -4, -6, and − 7 in PD-MSCs^{PRL-1} were significantly elevated, although IGFBP-3 and − 5 were reduced, compared to naïve. These data show that PD-MSCs^{PRL-1} upregulate expression of IGFBP-2, -4, and − 7, and may control these IGFBPs secretion (Fig. 3).

IGFBPs induced by PD-MSCs $^{PRL-1}$ inhibit adipogenesis via upregulation of FAK and downregulation of PI3K/AKT/mTOR signaling pathway

We confirmed increased expression of adipogenic-specific genes in OFs with GO patients was down-regulated by PD-MSCs^{PRL-1}. Moreover, protein expression of PPAR-γ in OFs derived from GO patients cocultured with PD-MSCs^{PRL-1} was decreased compared to naïve coculture (Fig. 4a, b). Although no apparent differences of TNF-α between naïve and cocultured groups, (Fig. 4d), leptin expression in PD-MSCs^{PRL-1} coculture was remarkably decreased compared with naïve coculture (Fig. 4c). To further investigate the mechanism of inhibitory effects of PD-MSCs^{PRL-1} on IGF-1 mediated signaling of adipogenesis, we analyzed the expression levels of PI3K/AKT/mTOR pathway members by western blot assay. Protein expression of phosphorylated PI3K, AKT, mTOR in OFs with GO patients cocultured with PD-MSCs^{PRL-1} was significantly downregulated compared to non-cocultivation. Interestingly, PD-

MSCs^{PRL-1} co-culture in OF cells also decreased phosphorylated PI3K, and downstream AKT and mTOR expression compared with naïve coculture (Fig. 4e). In general, integrins are transmembrane receptor that facilitate cell-extracellular matrix adhesion and can interact with IGFBPs. To confirm increased IGFBPs by PD-MSCs^{PRL-1} in OFs with GO patients contribute to regulate the adipogenic effect through integrin signaling pathway, we investigated the expression of ITGA4 and ITGB7, and downstream signaling factor of integrin, focal adhesion kinase (FAK), in normal and GO-derived OFs cocultured with PD-MSCs^{PRL-1}. mRNA expression levels of ITGA4 and ITGB7 in normal and GO-derived OFs cocultured with PD-MSCs^{PRL-1} were higher than those in non-cocultivation (Fig. 4f, g). Moreover, mRNA expression of FAK, which is downstream factor of ITGA4 and ITGB7, in normal and GO-derived OFs cocultured with PD-MSCs^{PRL-1} was significantly higher than those in non-cocultivation and naïve coculture (Fig. 4h). As shown in Fig. 4e, mRNA level of FAK was consistent with the protein level. These findings suggest that enhanced expression of IGFBPs by PD-MSCs^{PRL-1} promote ITGA4 and ITGB7 signaling which leads to FAK activation, and downregulate of P13K/AKT/mTOR signaling pathway, resulting in inhibition of adipogenesis in orbital fibroblasts (Fig. 5).

Discussion

Mesenchymal stem cells (MSCs) have immune modulatory capacities for autoimmune disease including Graves' ophthalmopathy (GO) [10]. Because medical therapies including corticosteroids and radiotherapy for patients with GO lead to side effects developing malignancies, molecular mechanisms in de novo adipogenesis of main symptoms have pivotal roles for therapeutic applications. Especially, PD-MSCs contained immunosuppressive effects on antigen presenting cells and secreted soluble factors. In previous reports, PD-MSCs have more immunological advantage that expression of HLA-G and cytokines of IL-2, IL-4, IL-13, and GM-CSF were higher compared to other MSCs including BM-MSCs and AD-MSCs [12]. However, the aging of MSCs resulted in limited self-renewal ability likewise age-associated decrease in cellular number and functions [20]. Therefore, gene modification using gene delivery systems overcomes their limited functions to provide the effective therapeutic efficacy of MSCs [21]. Recent report revealed that genetically modified MSCs overexpressing IL-35 had application to autoimmune diseases for overcome the complication of long-term immunosuppression [22]. Our previous study was generated for TERT overexpressing PD-MSCs using nonviral AMAXA system underlying the regulatory mechanisms of self-renewal [23].

Phosphatase of regenerating liver-1 (PRL-1) comprises a member of subgroups related protein tyrosine phosphatases contacting a C-ternimal prenylation motif [14]. C-terminal residues and cellular redox environments were controlled by enzyme activity of PRL-1 [24]. In oxidative stressed retina and photoreceptor, modulation of PRL-1 activity regulates redox conditions [16]. We hypothesized that PD-MSCs overexpressing PRL-1 (PD-MSCs^{PRL-1}, PRL-1+) regulate oxidative conditions and adipogenesis symptom in orbital fibroblast (OF) with GO patients would be decreased.

Because little is known about efficacies to evaluate inhibition of adipogenesis by PD-MSCs^{PRL-1} in OFs with GO patients, we further analyzed that function-enhancement of PRL-1 in PD-MSCs was generated using non-viral AMAXA system. OFs isolated from patient with GO are capable of adipocyte differentiation [3]. In orbital adipose tissues and in vitro OFs after differentiation from GO patients, enhanced adiponectin, leptin and PPAR-γ have positive correlations [25]. Previous reports demonstrated that enhanced IGF-1 expression was affected and activated PI3K by upregulating PPAR-γ in the orbital fatty connective of patients with GO [26]. In general, IGF binds to IGFBPs. Individual IGFBPs act to increase or attenuate IGF signaling pathway [27]. Recently, IGFBP2 prevents adipogenesis [28] as well as IGFBP3 interferes with PPAR-γ dependent processes to impair adipocyte differentiation [29]. Overexpressed IGFBP2 inhibits both lipogenesis and adipogenesis in visceral adipocytes and involves cellular surface association of IGFBP2 activating integrin signaling pathway [30]. Similarly, IGFBP4 controlled the expression of insulin and IGF1 on mice adipose tissue expansion [31]. Because we previously analyzed that naïve and PD-MSCs^{PRL-1} significantly secreted IGFBPs using multiplex cytokine array (data not shown), PD-MSCs^{PRL-1} secreted IGFBP2, 4, 7 and inhibit adipogenesis. Enhanced IGFBPs though ITGA4 and ITGB7 by secreted PD-MSCs^{PRL-1} declined PPAR-γ dependent processes via downregulated PI3K/AKT/mTOR activities, and inhibited adipogenesis.

Conclusions

In this study, we have shown that PD-MSCs modified with PRL-1 gene using nonviral transfection efficiently overexpressed PRL-1 protein, and maintained the phenotype and multilineage differentiation property of MSCs. PD-MSCs^{PRL-1} induced IGFBPs expression and inhibit adipogenesis via up-regulation of FAK and down-regulation of PI3K/AKT/mTOR signaling pathway in orbital fibroblasts with GO patients. In this study, to overcome the medical problems with GO patients, the functional enhancement of PD-MSCs by nonviral gene modification provides novel insight into next-generation MSC-based cell therapy for future clinical trials in immunological diseases.

Abbreviations

COL1A1:Collagen type 1 alpha 1; FABP4:Fatty acid-binding protein 4; FAK:Focal adhesion kinase; GFP:Green fluorescent protein; GO:Graves' ophthalmopathy; GVHD:Graft-versus-host-disease; IGF-1R:Insulin-like growth factor 1 receptor; ITGA4:Integrin alpha 4; LPL:Lipoprotein lipase; OC:Osteocalcin; OF:Orbital fibroblast; PD-MSCs:Placenta-derived mesenchymal stem cells; PPAR-γ:Peroxisome proliferator-activated receptor-gamma; PRL-1:Phosphatase of regenerating liver-1; TERT:Telomerase reverse transcriptase

Declarations

Acknowledgements

Not applicable.

Author’s contributions

JYK contributed to the analysis and interpretation of data and manuscript writing. H-JL did the data analysis. HL provided OF. SP and GJK reviewed the manuscript. GJK did financial support, and final approval of manuscript. All authors read and approved the final manuscript.

Funding

This research was supported by grants of the Korea Health Technology R&D Project through the Korea Health Industry Development Institute (KHIDI), funded by the Ministry of Health & Welfare, Republic of Korea (grant number : HI16C1599) and by Basic Science Research Program through the National Research Foundation of Korea (NRF) funded by the Ministry of Education (grant number: 2019R1I1A1A01057255).

Availability of data and materials

All data and materials are available upon request.

Ethics approval and consent to participate

The process of obtaining orbital adipose tissues was approved by the Institutional Review Board of Bundang CHA Medical Center (Seongnam, Republic of Korea), and placenta tissues were collected for research purposes by the Institutional Review Board of CHA Gangnam Medical Center (Seoul, Republic of Korea). All patients consented to the proper use for research.

Consent for publication

Not applicable

Competing interests

The authors declare that they have no competing interests.

Author details

[1]Department of Biomedical Science, CHA University, Seongnam 13488, Republic of Korea; [2]Center for Non-Clinical Development, CHA Advanced Research Institute CHA University, Seongnam 13488, Republic of Korea; [3]Department of Ophthalmology, CHA Bundang Medical Center CHA University, Seongnam 13496, Republic of Korea

References

1. Bahn RS. Graves' ophthalmopathy. N Engl J Med. 2010;362(8):726-38.

2. Mohyi M, Smith TJ. IGF1 receptor and thyroid-associated ophthalmopathy. J Mol Endocrinol. 2018;61(1):T29-T43.
3. Mimura LY, Villares SM, Monteiro ML, Guazzelli IC, Bloise W. Peroxisome proliferator-activated receptor-gamma gene expression in orbital adipose/connective tissues is increased during the active stage of Graves' ophthalmopathy. Thyroid. 2003;13(9):845-50.
4. Li B, Smith TJ. PI3K/AKT pathway mediates induction of IL-1RA by TSH in fibrocytes: modulation by PTEN. J Clin Endocrinol Metab. 2014;99(9):3363-72.
5. Ponto KA, Zang S, Kahaly GJ. The tale of radioiodine and Graves' orbitopathy. Thyroid. 2010;20(7):785-93.
6. Shams PN, Ma R, Pickles T, Rootman J, Dolman PJ. Reduced risk of compressive optic neuropathy using orbital radiotherapy in patients with active thyroid eye disease. Am J Ophthalmol. 2014;157(6):1299-305.
7. Giotaki Z, Fountas A, Tsirouki T, Bargiota A, Tigas S, Tsatsoulis A. Adrenal reserve following treatment of Graves' orbitopathy with intravenous glucocorticoids. Thyroid. 2015;25(4):462-3.
8. Moleti M, Giuffrida G, Sturniolo G, Squadrito G, Campenni A, Morelli S et al. Acute liver damage following intravenous glucocorticoid treatment for Graves' ophthalmopathy. Endocrine. 2016;54(1):259-68.
9. Mazonakis M, Tzedakis A, Lyraraki E, Damilakis J. Risk of developing radiogenic cancer following photon-beam radiotherapy for Graves' orbitopathy. Med Phys. 2018;45(10):4775-82.
10. De Miguel MP, Fuentes-Julian S, Blazquez-Martinez A, Pascual CY, Aller MA, Arias J, Arnalich-Montiel F. Immunosuppressive properties of mesenchymal stem cells: advances and applications. Curr Mol Med. 2012;12(5):574-91.
11. Jang MJ, Kim HS, Lee HG, Kim GJ, Jeon HG, Shin HS et al. Placenta-derived mesenchymal stem cells have an immunomodulatory effect that can control acute graft-versus-host disease in mice. Acta Haematol. 2013;129(4):197-206.
12. Lee JM, Jung J, Lee HJ, Jeong SJ, Cho KJ, Hwang SG, Kim GJ. Comparison of immunomodulatory effects of placenta mesenchymal stem cells with bone marrow and adipose mesenchymal stem cells. Int Immunopharmacol. 2012;13(2):219-24.
13. Rios P, Li X, Kohn M. Molecular mechanisms of the PRL phosphatases. FEBS J. 2013;280(2):505-24.
14. Si X, Zeng Q, Ng CH, Hong W, Pallen CJ. Interaction of farnesylated PRL-2, a protein-tyrosine phosphatase, with the beta-subunit of geranylgeranyltransferase II. J Biol Chem. 2001;276(35):32875-82.
15. Gao J, Liao J, Yang GY. CAAX-box protein, prenylation process and carcinogenesis. Am J Transl Res. 2009;1(3):312-25.
16. Yu L, Kelly U, Ebright JN, Malek G, Saloupis P, Rickman DW, McKay BS, Arshavsky VY, Bowes Rickman C. Oxidative stress-induced expression and modulation of Phosphatase of Regenerating Liver-1 (PRL-1) in mammalian retina. Biochim Biophys Acta. 2007;1773(9):1473-82.

17. Park M, Banga JP, Kim GJ, Kim M, Lew H. Human placenta-derived mesenchymal stem cells ameliorate orbital adipogenesis in female mice models of Graves' ophthalmopathy. Stem Cell Res Ther. 2019;10(1):246.
18. Lee MJ, Jung J, Na KH, Moon JS, Lee HJ, Kim JH et al. Anti-fibrotic effect of chorionic plate-derived mesenchymal stem cells isolated from human placenta in a rat model of CCl(4)-injured liver: potential application to the treatment of hepatic diseases. J Cell Biochem. 2010;111(6):1453-63.
19. Seok J, Jung HS, Park S, Lee JO, Kim CJ, Kim GJ. Alteration of fatty acid oxidation by increased CPT1A on replicative senescence of placenta-derived mesenchymal stem cells. Stem Cell Res Ther. 2020;11(1):1.
20. Li Y, Wu Q, Wang Y, Li L, Bu H, Bao J. Senescence of mesenchymal stem cells (Review). Int J Mol Med. 2017;39(4):775-82.
21. Nowakowski A, Walczak P, Lukomska B, Janowski M. Genetic Engineering of Mesenchymal Stem Cells to Induce Their Migration and Survival. Stem Cells Int. 2016;2016:4956063.
22. Guo H, Li B, Wang W, Zhao N, Gao H. Mesenchymal stem cells overexpressing IL-35: a novel immunosuppressive strategy and therapeutic target for inducing transplant tolerance. Stem Cell Res Ther. 2018;9(1):254.
23. Lee HJ, Choi JH, Jung J, Kim JK, Lee SS, Kim GJ. Changes in PTTG1 by human TERT gene expression modulate the self-renewal of placenta-derived mesenchymal stem cells. Cell Tissue Res. 2014;357(1):145-57.
24. Skinner AL, Vartia AA, Williams TD, Laurence JS. Enzyme activity of phosphatase of regenerating liver is controlled by the redox environment and its C-terminal residues. Biochemistry. 2009;48(20):4262-72.
25. Kumar S, Leontovich A, Coenen MJ, Bahn RS. Gene expression profiling of orbital adipose tissue from patients with Graves' ophthalmopathy: a potential role for secreted frizzled-related protein-1 in orbital adipogenesis. J Clin Endocrinol Metab. 2005;90(8):4730-5.
26. Zhao P, Deng Y, Gu P, Wang Y, Zhou H, Hu Y, Chen P, Fan X. Insulin-like growth factor 1 promotes the proliferation and adipogenesis of orbital adipose-derived stromal cells in thyroid-associated ophthalmopathy. Exp Eye Res. 2013;107:65-73.
27. Hwa V, Oh Y, Rosenfeld RG. The insulin-like growth factor-binding protein (IGFBP) superfamily. Endocr Rev. 1999;20(6):761-87.
28. Wheatcroft SB, Kearney MT, Shah AM, Ezzat VA, Miell JR, Modo M et al. IGF-binding protein-2 protects against the development of obesity and insulin resistance. Diabetes. 2007;56(2):285-94.
29. Chan SS, Schedlich LJ, Twigg SM, Baxter RC. Inhibition of adipocyte differentiation by insulin-like growth factor-binding protein-3. Am J Physiol Endocrinol Metab. 2009;296(4):E654-63.
30. Yau SW, Russo VC, Clarke IJ, Dunshea FR, Werther GA, Sabin MA. IGFBP-2 inhibits adipogenesis and lipogenesis in human visceral, but not subcutaneous, adipocytes. Int J Obes (Lond). 2015;39(5):770-81.

31. Gealekman O, Gurav K, Chouinard M, Straubhaar J, Thompson M, Malkani S, Hartigan C, Corvera S. Control of adipose tissue expandability in response to high fat diet by the insulin-like growth factor-binding protein-4. J Biol Chem. 2014;289(26):18327-38.

Figures

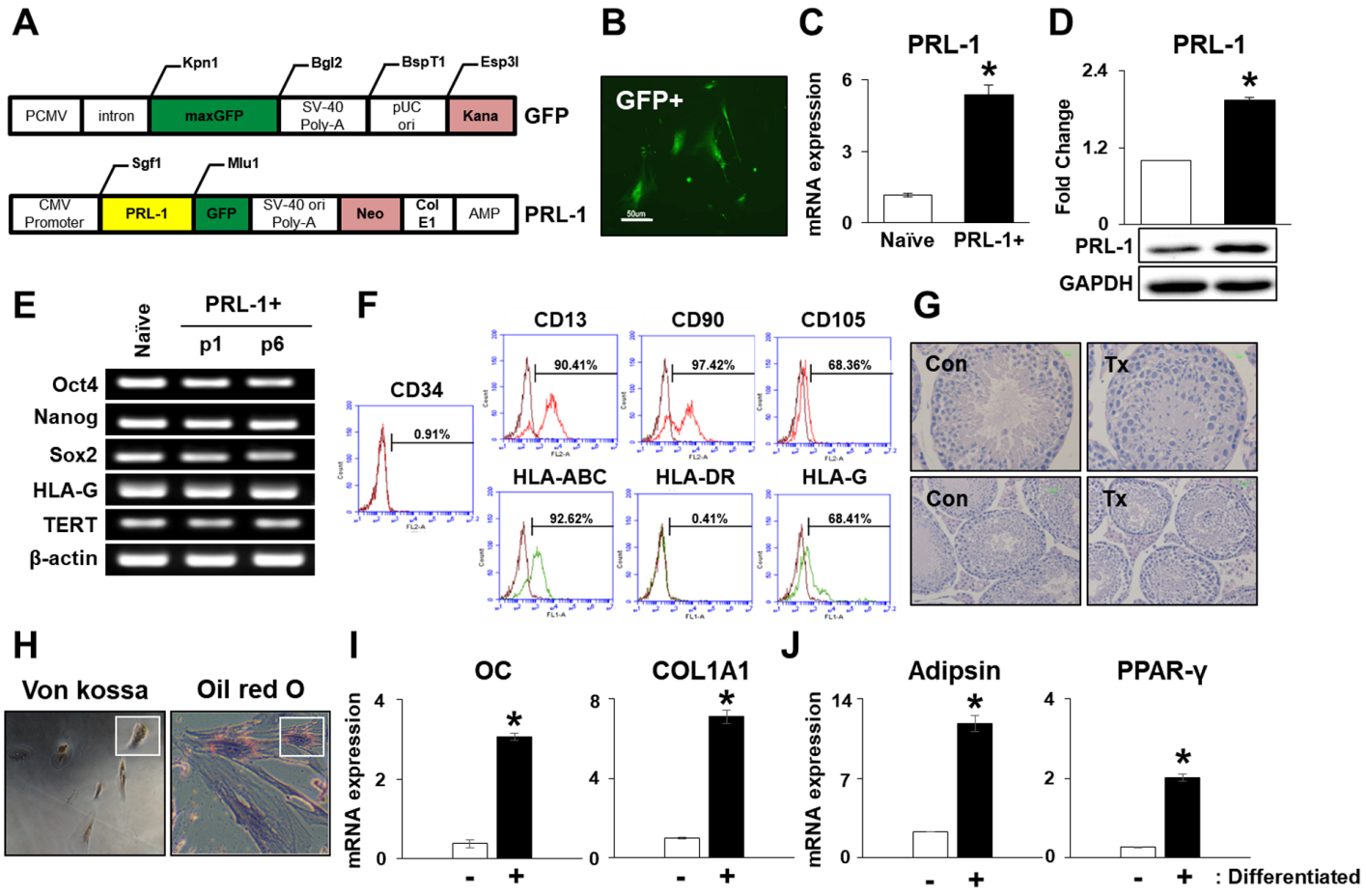

Figure 1

Characterization of PD-MSCs modified with PRL-1 gene. a GFP and PRL-1 plasmid vector map. b Expression of GFP in PD-MSCsPRL-1 using non-viral gene delivery system. Scale bars: 100 μm. c mRNA and d protein expressions of PRL-1 in PD-MSCsPRL-1 (mean ± SD *p < 0.05 compared with naïve). e Stemness markers in naïve and PD-MSCsPRL-1 depending on passages by RT-PCR. f Surface markers of hematopoietic, non-hematopoietic, and HLA family in PD-MSCsPRL-1 by FACS analysis. g Histopathological analysis of NOD/SCID mice testis and PD-MSCsPRL-1 transplanted in NOD/SCID mice testis after 14 weeks by H&E. h Osteogenic and adipogenic differentiations of PD-MSCsPRL-1 using von Kossa and Oil Red O staining. mRNA expression of i osteogenic- (OC and COL1A1) and j adipogenic-specific markers in differentiated PD-MSCsPRL-1 (mean ± SD *p < 0.05 compared with undifferentiated groups).

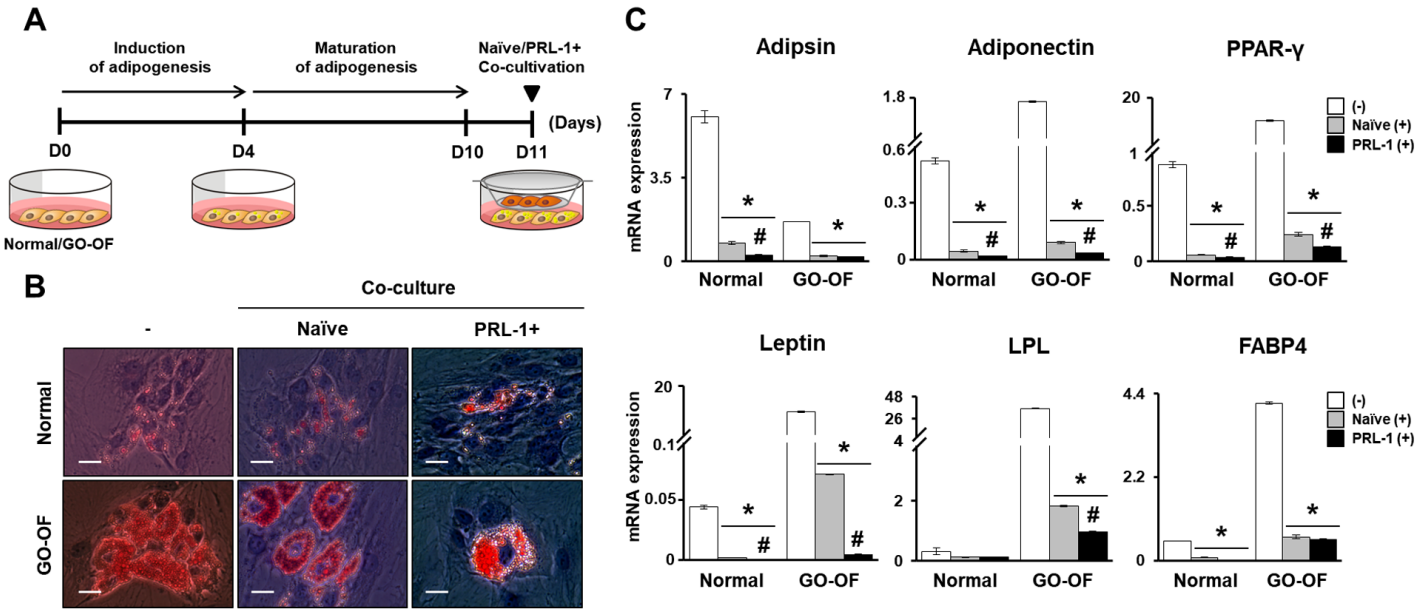

Figure 2

PD-MSCsPRL-1 inhibit adipogenesis OF with GO patients. a A schematic diagram describing the naïve and PD-MSCsPRL-1 cocultivation with adipogenesis differentiation in normal (n = 3) and OF with GO patients (n = 3). During the first 4 days, adipogenesis in normal and GO-derived OFs was induced. From 10 days, normal and GO-derived OFs were maintained for maturation of adipogenesis. For 24 h, naïve and PD-MSCsPRL-1 in transwell insert system were cocultured. b Representative images of adipogenic differentiation in normal and GO-derived OFs with naïve and PD-MSCsPRL-1 cocultivation. Scale bars: 100 μm. c qRT-PCR analysis of mRNA adipogenic specific markers in normal and GO-derived OFs induced adipogenic differentiation according to naïve and PD-MSCsPRL-1 cocultivation. (mean ± SD *p < 0.05 compared with non cocultivation groups) (mean ± SD #p < 0.05 compared with naïve cocultivation groups).

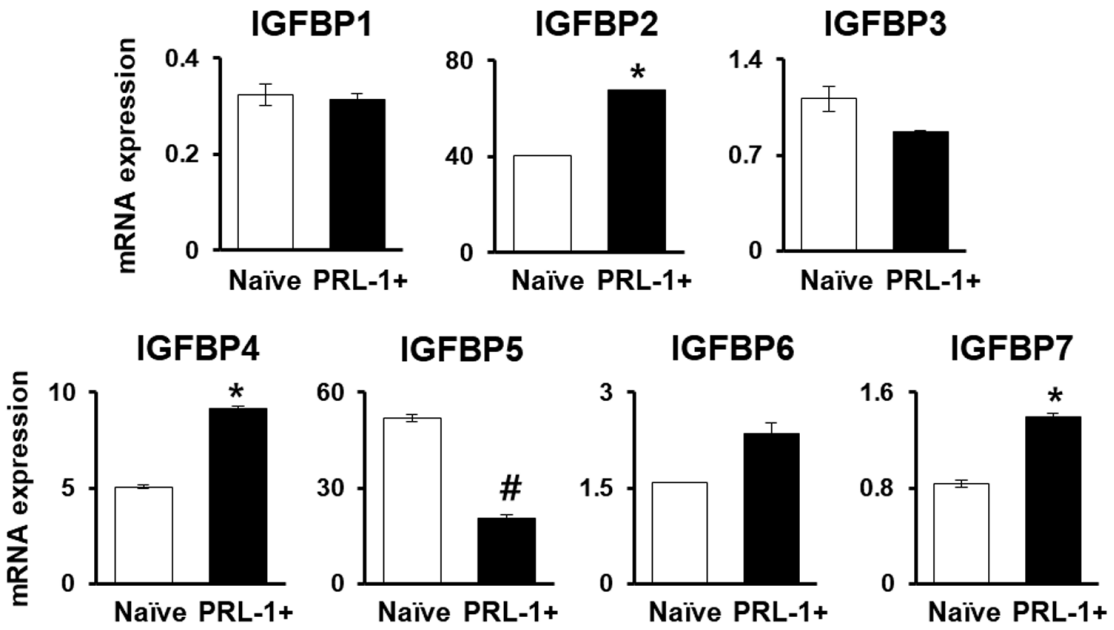

Figure 3

PD-MSCsPRL-1 promote expression of IGFBP genes. mRNA expression of IGFBPs in naïve and PD-MSCsPRL-1 using qRT-PCRs (mean ± SD *p < 0.05 compared with naïve) (mean ± SD #p < 0.05 compared with naïve).

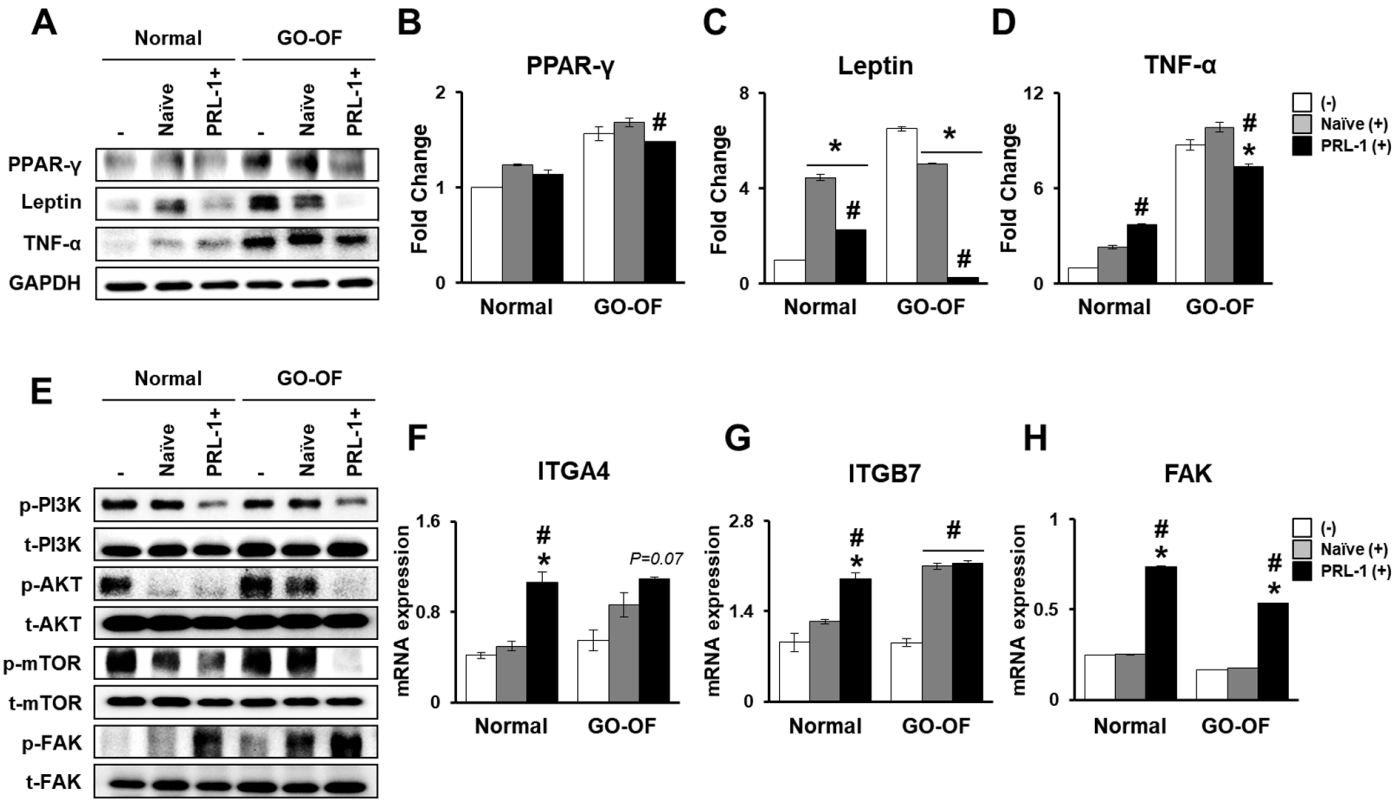

Figure 4

IGFBPs induced by PD-MSCsPRL-1 inhibit adipogenesis via upregulation of FAK and downregulation of PI3K/AKT/mTOR signaling pathway. a Protein expressions of PPAR-γ, Leptin, and TNF-α in normal and GO-derived OFs with naïve and PD-MSCsPRL-1 cocultivation after 24 h using western blotting. Quantitative analysis of b PPAR-γ c Leptin and d TNF-α in normal and GO-derived OFs with naïve and PD-MSCsPRL-1 cocultivation after 24 h (mean ± SD *p < 0.05 compared with non-cocultivation groups) (mean ± SD #p < 0.05 compared with naïve cocultivation groups). e Protein expressions of phospho/total-PI3K, AKT, mTOR, and FAK in normal and GO-derived OFs with naïve and PD-MSCsPRL-1 cocultivation after 24 h using western blotting. mRNA expression of f ITGA4, g ITGB7, and h FAK in normal and GO-derived OFs with naïve and PD-MSCsPRL-1 cocultivation after 24 h (mean ± SD *p < 0.05 compared with non-cocultivation groups) (mean ± SD #p < 0.05 compared with naïve cocultivation groups).

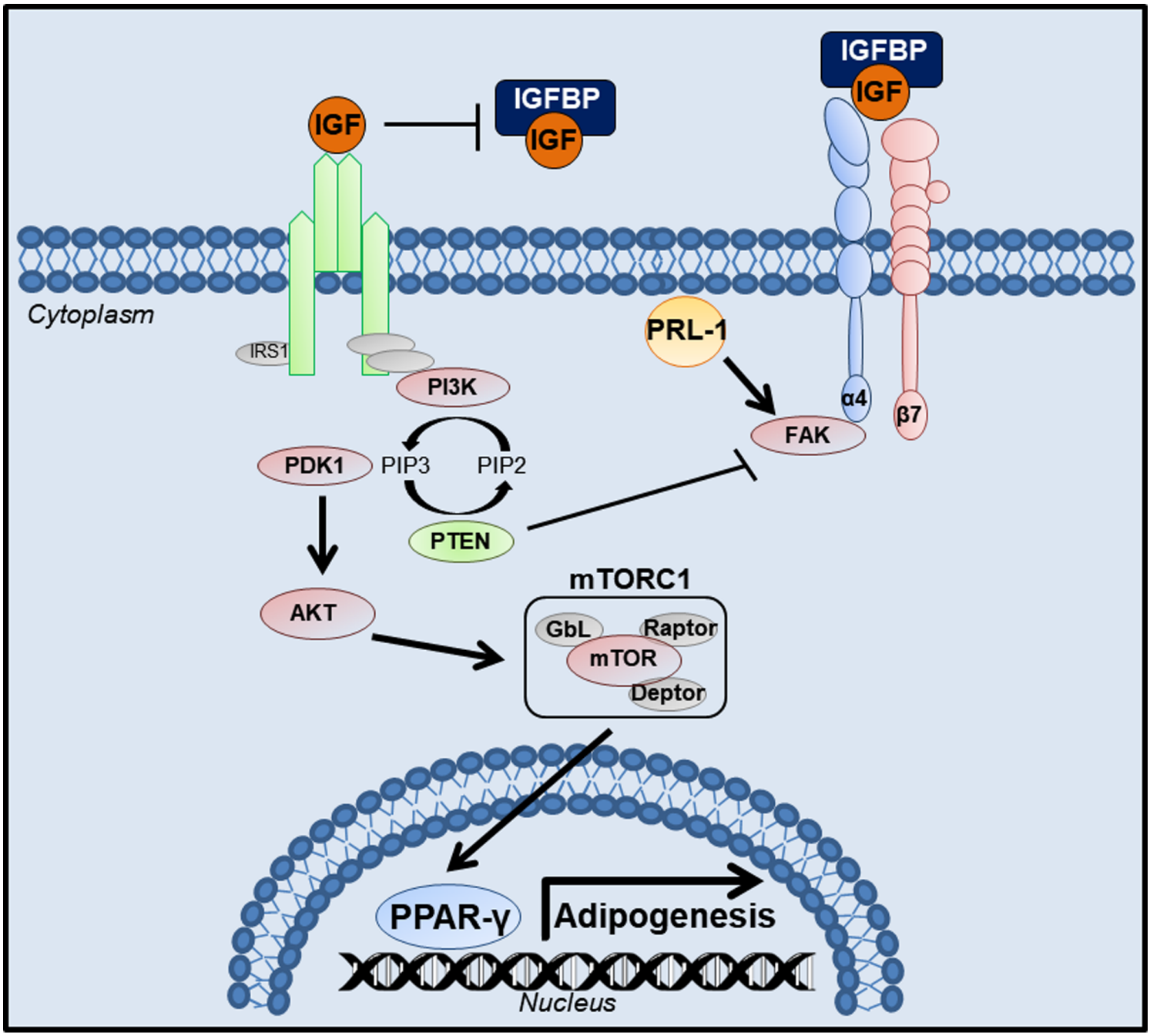

Figure 5

Summarized diagram proposes that anti-adipogenic key factor of secreted IGFBPs in PD-MSCsPRL-1 inhibit adipogenesis in OFs with GO patients through upregulation of FAK and downregulation of PI3K/AKT/mTOR signaling pathway.